UNIVERSITY OF BATH

University of Bath

Crystallization Fouling With Enhanced Heat Transfer Surfaces

B.D. Crittenden[1], M. Yang[1], L. Dong[1], R. Hanson[1], J. Jones[1], K. Kundu[1], J. Harris[1], Oleksandr Klochok[2], Olga Arsenyeva[2], and Petro Kapustenko[2]

[1]Department of Chemical Engineering, University of Bath, United Kingdom

[2]Spivdruzhnist-T JSC, Kharkiv, Ukraine

Address correspondence to Professor B. D. Crittenden, Department of Chemical Engineering,

University of Bath, Bath, BA2 7AY, United Kingdom, Tel: 0 (44) 1225 386501, Email:

cesbdc@bath.ac.uk

ABSTRACT

The aim of this paper is to demonstrate that a simple stirred batch cell can be used to study the effects of surface shear stress (amongst other process parameters) on fouling from saturated calcium salt solutions. For otherwise identical operating conditions, the overall fouling rate on a smooth mild steel surface was found to be reduced when either fine wires were attached to it or when helical threads were incorporated into the surface, either in the form of a continuous helical groove or in the form of a raised helix. The raised helical surface was more effective in reducing fouling than the helical groove. The results confirm the general effect that fouling rates can be reduced by increasing the surface shear stress through surface enhancement. A simple mathematical model has been developed to take into account the dynamic change in bulk concentration as crystallization fouling occurs. In all cases, the overall fouling resistance increased asymptotically towards a constant value and could easily and accurately be described quantitatively by the new analytical model. The variations of shear stresses on the various surfaces were determined from CFD simulations using the commercial package Comsol 4.2.

INTRODUCTION

Crystallization fouling on heat exchanger surfaces can create chronic operational problems in a broad range of processing applications that include cooling water systems, desalination, steam generation, etc. Energy losses, additional power consumption and the costs of cleaning all make this practical operational problem a significant challenge in the progression towards sustainable development.

Several researchers have investigated crystallization fouling of calcium sulfate and calcium carbonate using recirculating tubular flow type devices [1-4]. The effects of a number of operational parameters such as velocity, temperature, calcium concentration, and

surface geometry on the fouling rate have been studied. In the research presented in this paper, a different approach has been adopted. The simple stirred batch cell which was originally designed by Young et al. [5] to study fouling from crude oils has now been used for the first time to study the effects of surface shear stress and surface temperature on fouling from saturated calcium salt solutions. The principal advantage of the batch cell over its continuous flow counterpart is that different surface configurations that enhance turbulence and heat transfer can easily be studied. The effects of enhancements such as wires, dimples, helical threads, etc, on fouling can then be interpreted to assist prediction of the effects of surface enhancements on fouling in, for example, plate heat exchangers and tubes fitted with inserts such as hiTRAN. A disadvantage of the stirred batch cell, given that the volume of solution is small (about 1 litre), is that the concentration of calcium salt may not be considered to be constant due to the formation of crystalline deposits on the heated surface. The fouling rate is therefore dynamically related to the change in bulk concentration with time. This clearly sets a challenge when interpreting the experimental data but, on the other hand, initial fouling rates arise at the known initial bulk concentration and, of course, the data may provide an excellent opportunity to discover the effect of bulk concentration on fouling rate in a single simple experiment.

Apart from determining fouling resistances through interpretation of the heat transfer data, the actual fouling layer profiles have also been studied using a ProScan laser micro-scanning technology. In addition, the experimental data are complemented by computational fluid dynamics (CFD) simulations of the fluid flow in the stirred cell in the manner described elsewhere by Yang et al. [6]. The CFD studies have been made for test probes with and without surface enhancements using the commercial package Comsol 4.2. The resulting velocity, shear stress and temperature fields are able to show clearly how the experimental

effects of temperature and surface shear stress on the fouling are well correlated by the CFD simulations.

EXPERIMENTS

The stirred cell and probes

Details of the stirred cell system and the heated test probe shown in Figure 1 are provided by Young et al. [5]. The cell comprises a pressure vessel made in-house from a block of 304 stainless steel and is fitted with a top flange. The base of the vessel houses an upwards pointing test probe heated internally by a cartridge heater. The heat flux is controlled electrically. A batch of about 1.0 litres of aqueous solution is agitated by a downwards facing cylindrical stirrer mounted co-axially with the test probe and driven by an electric motor. External band heaters are incorporated to provide initial heating to the vessel and its contents. An internal cooling coil uses a non-fouling fluid (Paratherm) to remove heat at the rate that it is put in via the cartridge heater during the fouling run. The vessel is fitted with a pressure relief valve and there is a single thermocouple to measure the bulk solution temperature. The mechanisms for the control of bulk temperature and stirring speed are described elsewhere [5]. The surface temperature of the test probe can be changed by altering the heat flux by adjusting the input power to the cartridge heater.

Details of the plain mild steel probe and the one fitted with a nest of wires, as shown in Figure 2, have been reported elsewhere [7]. The probe has, additionally, been modified by attaching sleeves with helical threads incorporated into their surface, either in the form of a continuous helical groove or in the form of a raised helix. Figure 3 shows the two helically enhanced sleeves with negative and positive helices, respectively, and as a reference, a plain sleeve of the same diameter as the two helically enhanced ones.

Materials and experimental method

The purpose of this paper is to confirm that the stirred batch cell can be used to study the effects of enhanced surfaces on fouling from aqueous solutions. For this purpose, simple standard solutions of calcium sulfate and calcium carbonate have been used. This study is not concerned with studying the effects of water chemistry on the fouling process. The standard solution of $CaSO_4$ is prepared by dissolving 4.1g of $Ca(NO_3)_2$ and 8.0 g of $Na_2SO_4(H_2O)_{10}$ (both from Sigma-Aldrich) in 500 ml of deionized water, and then mixing the two solutions to form a 1 litre working solution containing 3400 ppm of $CaSO_4$ at pH=5.6. The standard solution of $CaCO_3$ is prepared by dissolving 1.68 g of $NaHCO_3$ and 1.44 g of $CaCl_2(H_2O)_2$ (both from Sigma-Aldrich) in 500 ml of deionized water, and then mixing the two solutions to form a 1 litre working solution containing 1000 ppm of $CaCO_3$ at pH=5.2. For working solutions at other concentrations, the mass of each chemical is adjusted proportionately. All chemicals are reagent grade. The working solution is transferred to the stirred batch cell and brought up to the desired bulk operating temperature by means of the external band heaters with the solution being stirred by the cell's internal rotor. Subsequently, the test probe is brought up to the desired surface temperature. The two heating sources and a PID-controlled cooling circulator work together and maintain the thermal steady state for the stirred cell. The operating conditions for data reported in this paper are provided in Table 1.

At the end of a fouling run, the stirred batch cell is cooled and the probe is removed. After drying, the probe is held within a V block and placed in the measuring plate of the ProScan 2000 instrument (Scantron Industrial Products Ltd, Taunton, UK). The surface of the probe is scanned using a laser optical sensor to measure the thickness profile of the fouling layer.

CFD SIMULATION

CFD and heat transfer simulations are carried out using Comsol Version 4.2a. The model geometry is set up to be three dimensional. The boundary conditions are wall functions for all solid-fluid boundaries, boundary layer heat sources for the cartridge heater and the band heaters, and variable temperature depending on the position from bottom to top for the cooling coil, respectively. The physical model is non-isothermal flow in a turbulent mode. Justification of the flow mode has been provided earlier by Yang et al. [6].

RESULTS AND DISCUSSION

Fouling resistance

The stirred batch cell is operated at constant bulk temperature and constant heat flux. Hence, as explained by Young et al. [5], the rate of fouling is directly proportional to the rate of change of surface temperature with time, with the assumption that as the deposit grows the film heat transfer coefficient remains constant.

Typical $CaSO_4$ curves for the difference between probe metal temperature and bulk temperature (for two thermocouple locations in one run) are shown in Figure 4. To convert the temperature difference to the fouling resistance, the heat flux at each thermocouple location needs to be determined instead of using the heat flux averaged over the whole of the probe surface. This is important because neither the surface temperature nor the heat flux is uniform vertically along the heated probe surface. The local heat flux can be obtained by means of CFD simulation. Figure 5 shows the CFD-predicted temperature field in the stirred cell and Figure 6 shows a comparison of the CFD-predicted surface temperatures with the measured values, thereby partially validating the CFD simulation.

Figure 7 shows the vertical profile of the heat flux over the probe surface. The local heat flux can also be determined using the heat transfer coefficient, which may be assumed to be

constant over the probe surface, given that it has been shown by Yang et al. [6] that the surface shear stress is relatively uniform over the probe surface when it is not enhanced. The local heat flux data were then used to calculate the fouling resistance using the temperature difference data such as that shown in Figure 4. Typical fouling curves in terms of how the fouling resistance varies with time are shown in Figures 8 and 9 for $CaSO_4$ and $CaCO_3$, respectively.

Effect of bulk concentration

Figures 8 and 9 show that the fouling resistances seem to reach asymptotic values relatively quickly. On the one hand, the net fouling rate which many consider to be the difference between a deposition rate and a removal rate can be considered to be reducing gradually towards zero up to the asymptote. On the other hand, further analysis reveals that this asymptotic situation could be caused by the gradual reduction in the driving force for crystallization as time progresses in the batch system. That is, as deposition progresses then the degree of super-saturation, due to the calcium salt leaving the bulk solution and depositing on the heated surface, causes a reduction in the bulk concentration. As an example of the potential magnitude of this concentration depletion effect, the dry mass of deposit after one fouling run was found to be 0.97 g, accounting for about 30% of the original salt mass in the bulk solution. If this is the cause of the asymptotic curves shown, for example, in Figures 8 and 9, then traditional asymptotic models may not be applicable and the dynamic change in bulk solution must, accordingly, be taken into account. Fahiminia et al. [2] developed a fouling rate model after Konak [8] and Krause [9] that gives a relationship between the initial fouling rate and the difference in concentration between super-saturation in the bulk and in normal saturation:

$$\emptyset = \frac{\Delta C}{\frac{1}{k_m} + \frac{1}{k_a^{1/n}} \emptyset^{(n-1)/n}} \tag{1}$$

Here Φ is the crystallization deposition rate, $\Delta C = (C_b - C_s)$ is the difference in concentration between the super-saturation in the bulk, C_b, and the normal saturation, C_s. Additionally, k_m, k_a, and n are the mass transfer coefficient, reaction rate constant, and reaction order, respectively. The fouling rate is related to Φ after Fahiminia et al. [2], as follows:

$$\frac{dR_f}{dt} = \frac{\emptyset}{\lambda_f \rho_f} \tag{2}$$

Here, λ_f and ρ_f are the thermal conductivity and density of the fouling deposit, respectively. Assuming that the bulk concentration reduction caused by fouling is proportional to the fouling resistance, then the change in bulk concentration is given by:

$$C_b = C_{b0} - \alpha R_f \tag{3}$$

In equation (3), C_{b0} is the initial bulk concentration and α is a constant. Given that $\Delta C_0 = (C_{b0} - C_s)$, then by combining equations (1), (2), and (3), by assuming that $n = 1$, and by taking into account a deposit removal term, as proposed by Crittenden et al. [10], equation (4) is obtained:

$$\frac{dR_f}{dt} = \frac{\frac{\Delta C_0}{\lambda_f \rho_f} - \frac{\alpha}{\lambda_f \rho_f} R_f}{\frac{1}{k_m} + \frac{1}{k_a}} - \gamma R_f \tag{4}$$

Here γ is the rate constant of any deposit removal process which would depend critically on both temperature and velocity (or surface shear stress). The equation is broadly similar to that developed for a model organic fluid system by Crittenden et al. [10]. Integration of equation (4) yields:

$$R_f = \frac{\Delta C_0}{\alpha + \frac{k_m + k_a}{k_m k_a} \gamma \lambda_f \rho_f} [(1 - \exp\left(-\left(\frac{\alpha}{\lambda_f \rho_f} \frac{k_m k_a}{(k_m + k_a)} + \gamma\right) t\right)] \tag{5}$$

As shown in Figures 8 and 9, the calcium salt fouling curves obtained using the stirred cell are correlated well using equation (5). The equation shows correctly that R_f is zero at $t = 0$, and that the fouling resistance tends towards a constant value when the running time is

sufficient, appearing to give a fouling curve of the asymptotic type. The maximum value of R_f is proportional to the difference in concentration between the initial bulk super-saturation and the normal saturation. The initial fouling rate can be obtained by differentiation of equation (5), setting $t = 0$, or simply using equation (4) and setting $R_f = 0$, at $t = 0$:

$$\frac{dR_f}{dt} = \frac{\Delta C_0}{\lambda_f \rho_f} \frac{k_m + k_a}{k_m k_a} \tag{6}$$

According to equation (6), the initial fouling rate is proportional to the initial difference in concentration between the initial super-saturation and the normal saturation. Figure 10 shows four initial fouling rates for $CaSO_4$ at different initial concentrations, keeping all other operating parameters constant. Figure 10 indeed shows that the initial fouling rate is linearly dependent on the difference in concentration between the initial super-saturation and the normal saturation, as given by equation (6).

Effect of temperature

In general, fouling is more intensive when the surface temperature is higher. As shown in Figures 5 and 6, the surface temperature of the heated probe is higher in the middle and lower towards its two ends. This variation arises as a result of the complex fluid flow patterns within the inner boundary of the batch cell's stirrer.

Figure 11 shows a photograph of the probe with a scaling deposit, and Figure 12 shows the deposit thickness profile along the vertical length obtained using ProScan 2000. It can be seen that the fouling layer thickness profile over the probe surface is strikingly similar in form to the temperature profile shown in Figure 6, with maxima in both deposit thickness and temperature occurring near to the middle of the heated probe surface. As reported previously by Yang et al. [6], the shear stress over the probe surface where the fouling zone is located is relatively constant. Hence the profile of the fouling behaviour is determined solely by the surface temperature and not the shear stress. Accordingly, the similarity of the temperature

and the fouling layer thickness profiles can be used to explain qualitatively the fouling rate behaviour in the experiment as a function of surface temperature.

Effect of surface enhancements on fouling

The overall fouling rate on a mild steel surface was found to be reduced when fine wires were attached to it. Under the same operational conditions of bulk temperature (55°C), initial surface temperature (88°C) and stirrer speed (300 rpm), the fouling rates on the wired probe and the bare probe were 2.9 x 10^{-5} m^2 K J^{-1}, and 4.2 x 10^{-5} m^2 K J^{-1}, respectively. Furthermore, as shown in Figure 13, the fouling rates on the probes fitted with helical surfaces (both negative and positive) were found to be lower than on the smooth surface. Moreover, the fouling rates on the positive helical surface were found to be the lowest. These reductions in fouling rate with enhanced surfaces are caused by the enhanced turbulence created either by the attached wires or by the incorporated helical threads. As shown in Figure 14, the shear stress is higher over the surface of the wired probe than over the bare probe. In the cases of probes fitted with sleeves, the average shear stress was found to increase in the order of smooth surface, negative helical groove, and positive helical surface, as shown in Figure 15. The difference in fouling rate on the different surface configurations can therefore be explained using the shear stress data obtained by CFD simulation.

It can be seen from Figure 16 that when wires are present the distribution of fouling is non-uniform. Indeed, the greatest amount of fouling appears downstream of the wires where the surface shear stress is the lowest (Figure 14) and the least amount appears just upstream of the wires where the surface shear stress is the highest. Given the clockwise flow direction, the shear stress is higher in front of a wire than behind it. This may suggest that fouling is more likely behind the wire, and this is confirmed by Figure 16.

At present it is not possible to measure surface shear stresses directly in the stirred cell. Nonetheless, values of the shear stress obtained by CFD simulation can be compared with

those inside a round tube. This leads to the concept of equivalent velocity first proposed by Yang et al. [6] which is the velocity inside a round tube that gives the same surface shear stress as in the geometry under study (here, the batch stirred cell). In the present case, the equivalent tube flow velocity of water lies in the range 0.05 to 0.5 m s^{-1} for the shear stress levels shown in Figure 15.

Figure 17 shows that the data obtained from Figures 13 and 15 seem to confirm that, for otherwise similar operating parameters including stirrer speed, there is a single correlation of initial fouling rate against surface shear stress that unifies the smooth surface and the two spirally enhanced surfaces. Although there is a limited amount of data from the three surfaces, the single correlation shows clearly the value in maintaining a high surface shear stress in crystallization fouling from calcium salts, whatever the method is to create the high shear stress on the heat transfer surface.

CONCLUSION

The stirred batch cell fouling has been used to make preliminary investigations of the effects of surface shear stress, surface temperature, and starting bulk concentration on calcium sulfate and calcium carbonate fouling. The paper demonstrates the flexibility and adaptability of the cell over its continuous flow counterpart, thereby offering a facility in which ways to mitigate fouling problems can be studied quickly. The potential weakness of the stirred batch cell is that it cannot be operated at steady state conditions. Hence, a model has been developed to take into account the dynamic change in bulk concentration as scaling occurs. The experimental results show that calcium salt scaling can be mitigated to some extent by changing the turbulence structure by means of attaching wires or incorporating helical threads into the heat transfer surface. This augurs well for mitigation of scaling by adding inserts into tubular flow systems or by surface corrugation. The scaling behaviour can

only be interpreted properly with the help of CFD simulation since it is essential that an understanding of the effect of shear stress is available. Given that the work reported in this paper focuses only on developing a methodology for interpreting fouling data in a stirred batch cell as well as on the effects of enhanced surfaces, the effect of the chemistry of calcium salt solutions has not been addressed here, but could be the subject for further research. Nevertheless, for otherwise similar operating conditions, it seems that there is a single correlation between initial fouling rate from calcium salt solutions and the shear stress at the heat transfer surface, irrespective of what the surface geometry is.

NOMENCLATURE

C $CaSO_4$ concentration, g/L or kg m^{-3}

C_b $CaSO_4$ bulk concentration, kg m^{-3}

C_{b0} $CaSO_4$ initial bulk concentration, kg m^{-3}

C_s $CaSO_4$ saturation concentration, kg m^{-3}

ΔC $(C_b - C_s)$, kg m^{-3}

ΔC_0 $(C_{b0} - C_s)$, kg m^{-3}

k_a surface reaction/attachment rate constant, m^4 kg^{-1} s^{-1}

k_m mass transfer coefficient, m s^{-1}

n reaction order

R_f fouling resistance, $m^2 \, K \, W^{-1}$

t time, s and hour

Greek symbols

α model constant, $kg \, m^{-5} \, K^{-1} \, W$

ρ_f fouling deposit density, $kg \, m^{-3}$

λ_f fouling deposit thermal conductivity, $W \, m^{-1} \, K^{-1}$

γ deposit removal rate coefficient, s^{-1}

Φ deposition flux, $kg \, m^{-2} \, s^{-1}$

REFERENCES

[1] Malayeri, M. R., and Müller-Steinhagen, H., Initiation of $CaSO_4$ scale formation on heat transfer surface under pool boiling conditions, *Heat Transfer Engineering*, vol. 28(3), pp. 240- 247, 2007.

[2] Fahiminia, F., Watkinson, A. P. and Epstein, N., Calcium sulfate scaling delay times under sensible heating conditions, in *Proceedings of the 6th International Conference on Fouling and Cleaning in Heat Exchangers*, Tomar, Portugal, July 1-6, ECI Symposium Series, vol. RP2, pp. 176-184, 2007.

[3] Albert, F., Augustin, W., and Scholl, S., Enhancement of heat transfer in crystallization fouling due to surface roughness, in *Proceedings of Eurotherm Conference on Fouling and Cleaning in Heat Exchangers*, Schladming, Austria, June 14-19, pp. 303-310, 2009.

[4] Esawy, M., Malayeri, M. R., and Müller-Steinhagen, H., Crystallization fouling of finned tubes during pool boiling: effect of fin density, *Proceedings of Eurotherm Conference on*

Fouling and Cleaning in Heat Exchangers, Schladming, Austria, June 14-19, pp. 311-318, 2009.

[5] Young, A., Venditti, S., Berrueco, C., Yang, M., Waters, A., Davies, H., Hill, S., Millan, M., and Crittenden, B. D., Characterisation of crude oils and their fouling deposits using a batch stirred cell system, *Heat Transfer Engineering*, vol. 32 (3-4), pp. 216-227, 2011.

[6] Yang, M., Young, A., and Crittenden, B. D., Use of CFD to correlate crude oil fouling against surface temperature and surface shear stress in a stirred fouling apparatus, *Proceedings of Eurotherm Conference on Fouling and Cleaning in Heat Exchangers*, Schladming, Austria, June 14-19, pp. 272 – 280, 2009.

[7] Yang, M., Wood, Z., Rickard, B., Crittenden, B., Gough, M., Droegemueller, P., and Higley, T., Mitigation of crude oil fouling by turbulence enhancement in a batch stirred cell, *Applied Thermal Engineering*, vol. 54, pp. 516-520, 2013.

[8] Konak, A. R., A new model for surface reaction controlled growth of crystals from solution, *Chem. Eng. Sci.,* vol 29, pp. 1537-1543, 1974.

[9] Krause, S., Fouling of heat transfer surface by crystallization and sedimentation, *International Chemical Engineering,* vol. 33, pp. 355-401, 1993.

[10] Crittenden, B.D., Kolaczkowski, S. T., and Hout, S. A., Modelling hydrocarbon fouling, *TransIChemE*, vol. 65, pp. 171-179, 1987.

[11] Calmanovici, C. E., Gabas, N., and Laguerle, C., Solubility measurement for calcium sulfate dehydrate in acid solution at 20, 50, and 70°C, *J. Chem. Eng. Data*, vol. 38, pp. 534-536, 1993.

Table 1 Operating Parameters

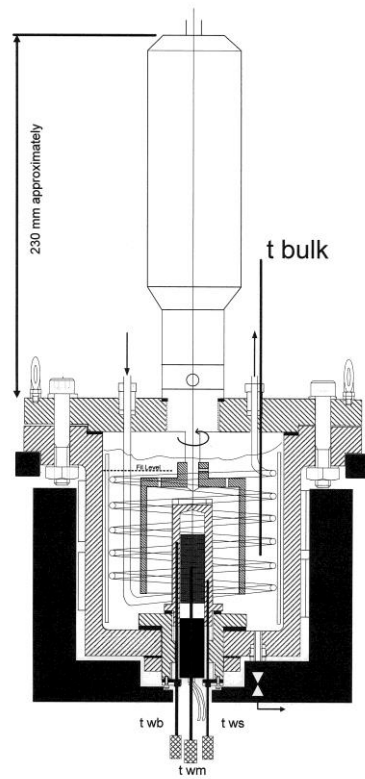| Operational parameter	Range
Bulk temperature (°C)	50 - 60
Average heat flux (kW m^{-2})	15 - 152
Surface temperature (°C)	70 - 95
Stirring speed (rpm)	60 - 400
Pressure (bar)	1 – 1.5

List of Figure Captions

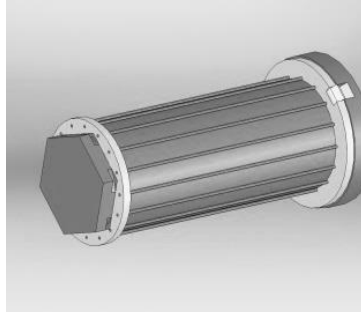Fig. 1 The stirred batch cell

twb, twm, and tws are thermocouples

Fig. 2 A fouling probe fitted with a nest of wires [7]

Fig. 3 Probe sleeves

a: Sleeve with negative helical thread

b: Sleeve with positive helical thread

c: Plain sleeve

Fig. 4 Typical fouling curve for a stainless steel probe

Symbols: temperature by twm; line: temperature by twb

Stirrer speed: 150 rpm; Bulk temperature: 55°C; Average heat flux: 31 kWm^{-2}

Fig. 5 Temperature field in the stirred cell

Heater power: 130 W; Stirrer speed: 300 rpm; Bulk temperature: 55°C

Temperature scale in K

Fig. 6 Vertical temperature profiles over the probe surface and over the vertical line where thermocouples are located.

Dashed line: probe surface temperature by simulation;

Solid line: temperature over the vertical line where the thermocouples located by simulation;

■: temperature reading by twm; ♦: temperature reading by twb

Stirrer speed: 130 rpm; Bulk temperature: 55°C; Average heat flux: 31 kW m^{-2}

Fig. 7 Heat flux profile over the probe surface

(stainless steel probe)

Heating power: 130W; Stirrer speed: 310 rpm; Bulk temperature: 55°C

Fig. 8 Fouling resistance data of $CaSO_4$ and model fit (stainless steel probe)

Symbols: experimental data derived from twb; Line: model fitting

Stirrer speed: 150 rpm; Bulk temperature: 55°C; Average heat flux: 32 kW m^{-2}

Fig. 9 Fouling resistance data of $CaCO_3$ and model fit (stainless steel probe)

Symbols: experimental data derived from twb; Thin line: model fitting

Stirrer speed: 150 rpm; Bulk temperature: 55°C; Average heat flux: 33 kW m^{-2}

Fig. 10 Linear dependency of initial fouling rate on the difference in concentration between initial super-saturation and normal saturation

$\Delta C_0 = (C_{b0} - C_s)$

with $C_s = 2.070$ kg m^{-3} from Calmanovici et al. [11]

Fig. 11 Mild steel probe with $CaSO_4$ deposit

Fig. 12 ProScan deposit thickness profile

Fig. 13 Fouling rates of $CaCO_3$ on smooth, negative and positive helical surfaces

Bulk temperature: 55°C

Fig. 14 Comparison of shear stress over the wired probe surface – around a circle ($0 - 2\pi$)

Stirrer speed: 200 rpm; Bulk temperature: 55°C

Upper curve: shear stress over wired probe

Lower curve: shear stress over bare probe

Fig. 15 Average shear stress on smooth surface, negative and positive helical surfaces

Fig. 16 Photograph of the wired probe after $CaSO_4$ fouling test; fluid flows clockwise when viewed from the top

Fig.17 Single correlation of initial fouling rate against surface shear stress

230 mm approximately

t bulk

t wb   t ws

t wm

Fig. 1 The stirred batch cell

twb, twm, and tws are thermocouples

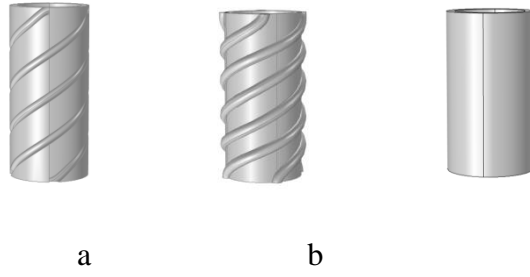Fig. 2 A fouling probe fitted with a nest of wires [7]

Fig. 3 Probe sleeves

a: Sleeve with negative helical thread; b: Sleeve with positive helical thread; c: Plain sleeve
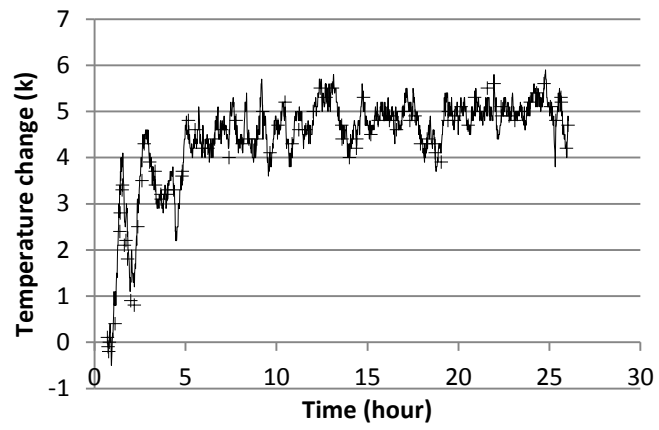
Fig. 4 Typical fouling curve for a stainless steel probe

Symbols: temperature by twm; Line: temperature by twb

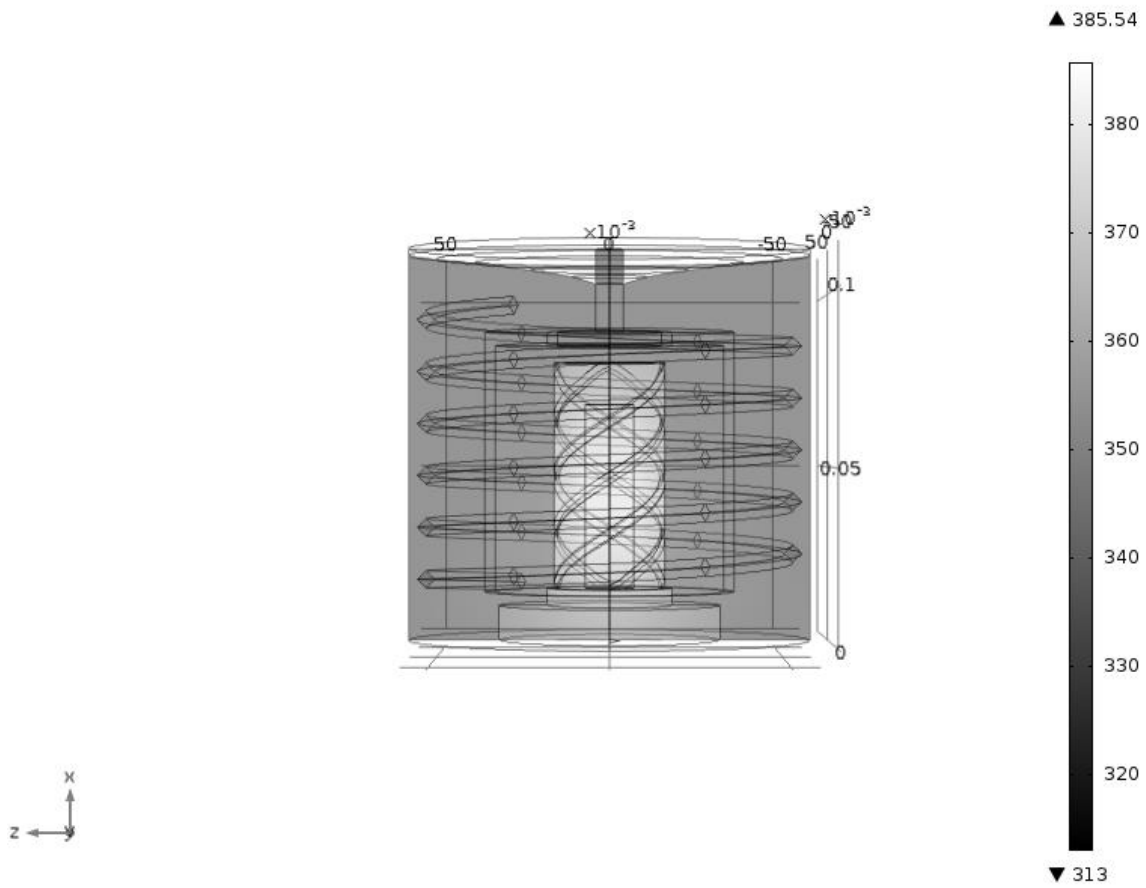Stirrer speed: 150 rpm; Bulk temperature: 55°C; Average heat flux: 31 kWm^{-2}

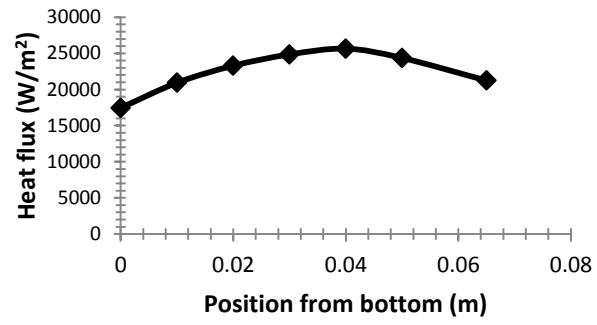Fig. 5 Temperature field in the stirred cell

Heater power: 130 W; Stirrer speed: 300 rpm; Bulk temperature: 55°C

Temperature scale in K

Fig. 6 Vertical temperature profiles over the probe surface and over the vertical line where

thermocouples are located.

Dashed line: probe surface temperature by simulation;

Solid line: temperature over the vertical line where the thermocouples located by simulation;

■: temperature reading by twm; ♦: temperature reading by twb

Stirrer speed: 130 rpm; Bulk temperature: 55°C; Average heat flux: 31 kW m^{-2}

Fig. 7 Heat flux profile over the probe surface

(stainless steel probe)

Heating power: 130W; Stirrer speed: 310 rpm; Bulk temperature: 55°C

Fig. 8 Fouling resistance data of $CaSO_4$ and model fit (stainless steel probe)

Symbols: experimental data derived from twb; Line: model fitting

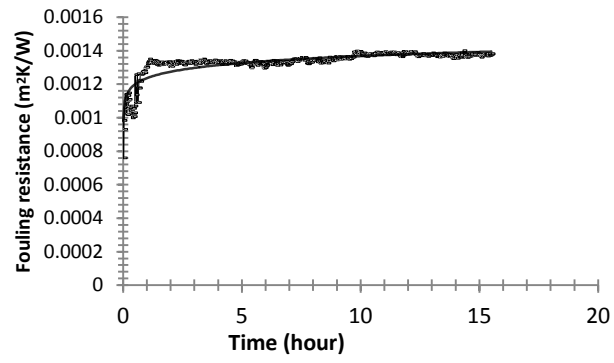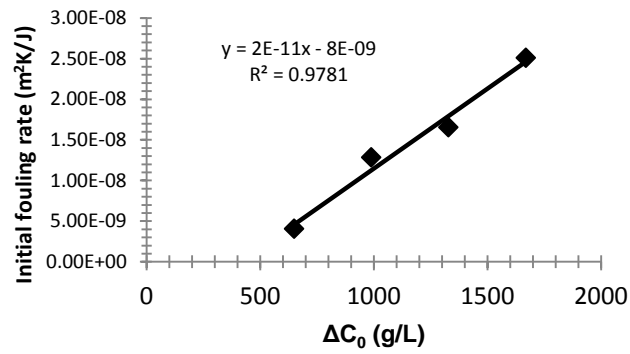Stirrer speed: 150 rpm; Bulk temperature: 55°C; Average heat flux: 32 kW m^{-2}

Fig. 9 Fouling resistance data of CaCO$_3$ and model fit (stainless steel probe)

Symbols: experimental data derived from twb; Thin line: model fitting

Stirrer speed: 150 rpm; Bulk temperature: 55°C; Average heat flux: 33 kW m^{-2}

Fig. 10 Linear dependency of initial fouling rate on the difference in concentration between

initial super-saturation and normal saturation

$$\Delta C_0 = (C_{b0} - C_s)$$

with $C_s = 2.070$ kg m^{-3} from Calmanovici et al. [11]
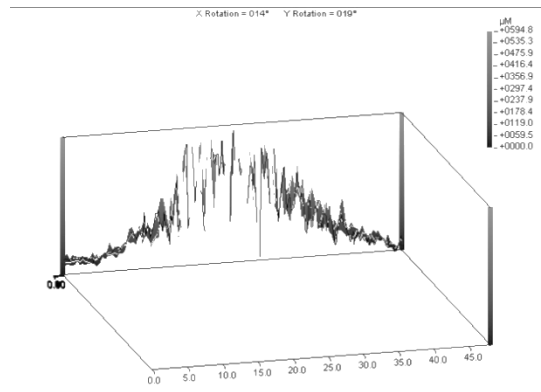
Fig. 11 Mild steel probe with CaSO$_4$ deposit

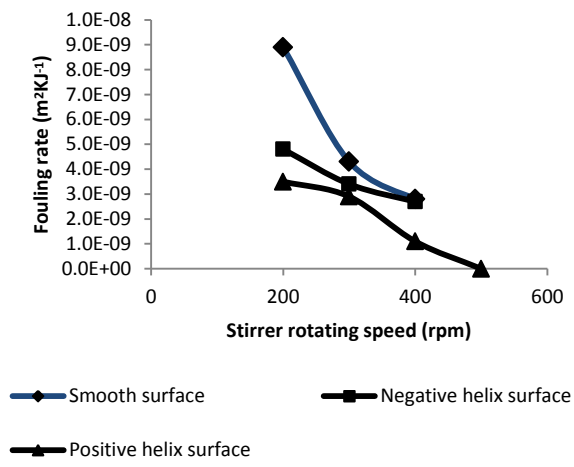Fig. 12 ProScan deposit thickness profile

Fig. 13 Fouling rates of CaCO$_3$ on smooth, negative and positive helical surfaces

Bulk temperature: 55°C
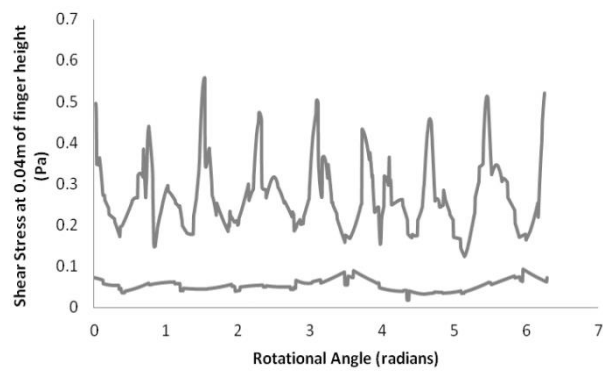
Fig. 14 Comparison of shear stress over the wired probe surface – around a circle (0 - 2 π)

Stirrer speed: 200 rpm; Bulk temperature: 55°C

Upper curve: shear stress over wired probe

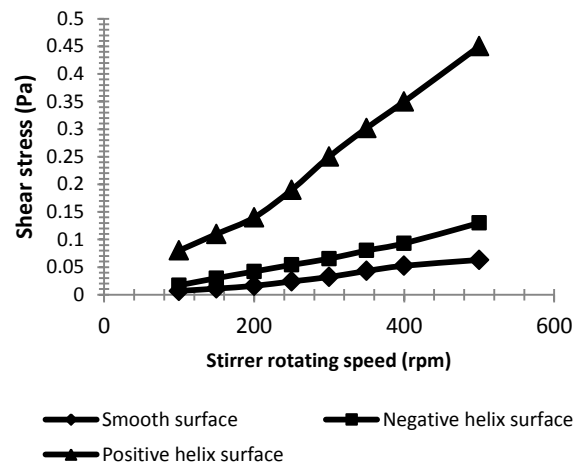Lower curve: shear stress over bare probe

Fig. 15 Average shear stress on smooth surface, negative and positive helical surfaces

Fig. 16 Photograph of the wired probe after CaSO$_4$ fouling test; fluid flows clockwise when viewed from the top
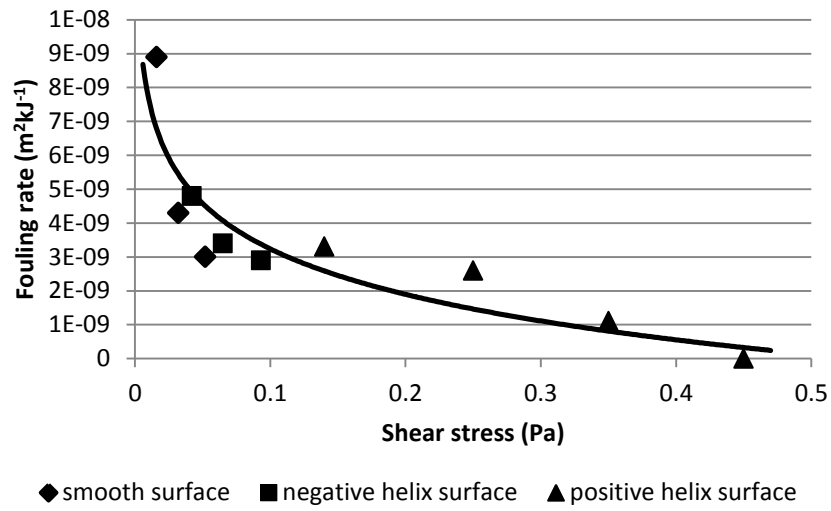
Fig.17 Single correlation of initial fouling rate against surface shear stress

Barry Crittenden is Professor of Chemical Engineering at the University of Bath and Leader of its Advanced Materials and Porous Solids research group. He is a Fellow of both the Royal Academy of Engineering and the Institution of Chemical Engineers. His research interests include activated carbon monoliths for environmental control and resource recovery, as well as hydrocarbon fouling in refinery heat exchangers.

Dr Mengyan Yang is a Senior Research Officer in the Department of Chemical Engineering at the University of Bath. He received his PhD in chemical engineering at Bath in 1993 after which he continued with post-doctoral research before joining Davisco Foods International, Minnesota, USA, as a Senior Scientist. He rejoined Bath in 2007 to pursue research in the field of crude oil fouling.

Dr Leilei Dong spent many years carrying out research on enhanced oil recovery at the University of Bath before taking up the appointment as a Design Engineer at HiETA Technology Ltd on the development of efficient and clean energy conversion and utilisation technologies. Lellei has many years of research and industrial experience in clean combustion and heat transfer enhancement.

Rob Hanson graduated with a first class MEng in Chemical Engineering at the University of Bath. As part of his degree he spent a year as a Utilities Engineer with ExxonMobil and now works as an Engineer with Croda Chemicals Ltd at Leek in Staffordshire.

Jack Jones graduated with a first class MEng in Biochemical Engineering at the University of Bath. Having travelled and worked as a volunteer in India for Frank Water Projects and Gram Vikas, he is now working as an Industrial Process Engineer for Environmental Water Services in Adelaide, Australia.

Krish Kundu is currently an undergraduate student studying for an MEng degree in Chemical Engineering at the University of Bath.

Jonathan Harris graduated with an MEng in Chemical Engineering at the University of Surrey. Having just completed research for an MPhil at the University of Bath, he now works for Heat Transfer Research Incorporated (HTRI), College Station, Texas, USA.

Oleksandr Klochok is currently engineer in the Spivdruzhnist-T JSC, Kharkiv, Ukraine. He graduated from National Technical University "Kharkiv Polytechnic Institute" (NTU KhPI) in 2010.

Dr. Olga Arsenyeva is a Senior Researcher in the Spivdruzhnist-T JSC, Kharkiv, Ukraine. She received her PhD in chemical engineering at National Technical University "Kharkiv Polytechnic Institute" (NTU KhPI) in 2004 after which she also works part time as an Associate Professor of NTU KhPI. Her research interests include heat transfer enhancement in plate heat exchangers accounting for fouling, as well as process integration for energy saving and pollution reduction.

Petro Kapustenko is General Director of Spivdruzhnist-T JSC, Kharkiv, Ukraine. On a part time basis he is also Professor of Chemical Engineering at the National Technical University "Kharkiv Polytechnic Institute" (NTU KhPI). His research interests include intensified heat transfer in plate heat exchangers, process integration for environmental control and energy saving, as well as water fouling in heat exchangers for process industry and district heating applications.